Chapter 4

Nonlinear Tests of One-Dimensional Closures

The linear theory of Landau-fluid equations works very well, and improves with the number of moments used. A relevant question, however, is whether the fluid equations can reproduce second-order nonlinear effects, such as ion Compton scattering. Mattor (1992) has questioned the ability of Landau-fluid equations to reproduce this effect near marginal stability. The analysis of Compton scattering is inherently 3D. However, the essential nature of the approximation of the second-order propagator can be illustrated in the simple exactly solvable one-dimensional problem of electron plasma echoes.

Plasma echoes (Gould et al. 1967) are an effect that can occur in highly collisionless plasmas due to the Hamiltonian nature of flows in phase space. Spatial perturbations that appear to have decayed have in reality become convoluted in phase space and disappeared in an averaged sense only. In some circumstances, additional perturbations can interact with the existing convoluted perturbations to produce a second-order perturbation that unfolds in time to produce a response much later, *the echo*. The simplest possible derivation of an electron plasma echo is presented here. There is an exact kinetic solution for this problem. The problem is solved using a finite moment system with closure and compared to the exact solution. An estimate for the number of moments required to accurately model second-order effects is therefore obtained. Finally the form of the second-order propagator obtained from the moment system is computed to illustrate the nature of the approximation being made.

4.1 Plasma Echoes

Plasma wave echoes (Gould et al. 1967; O'Neil and Gould 1968) are a second-order effect arising in the one-dimensional Vlasov equation. If the plasma is perturbed at a given wavelength, a density perturbation is excited and will die away due to

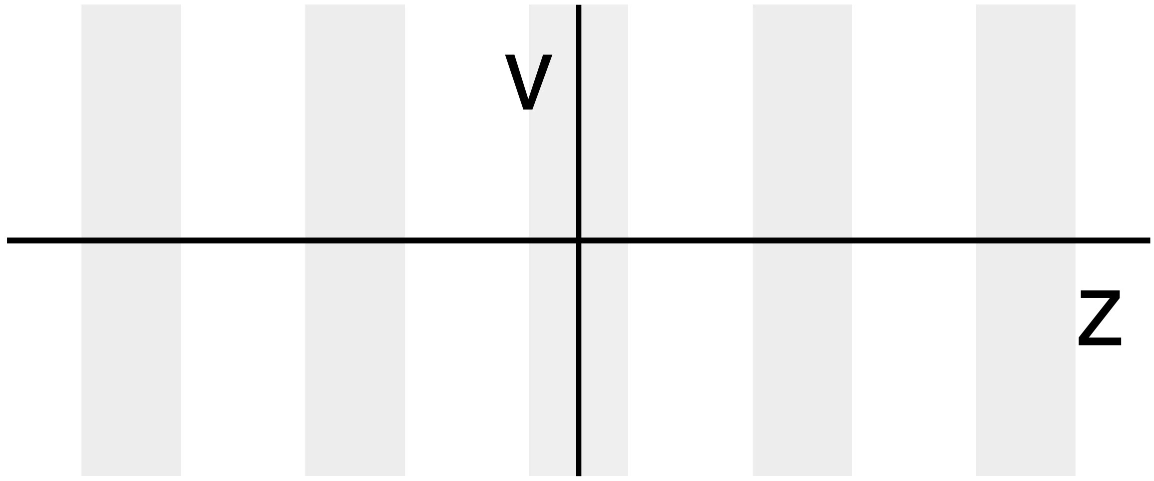

Initial perturbation with $k = 3$.

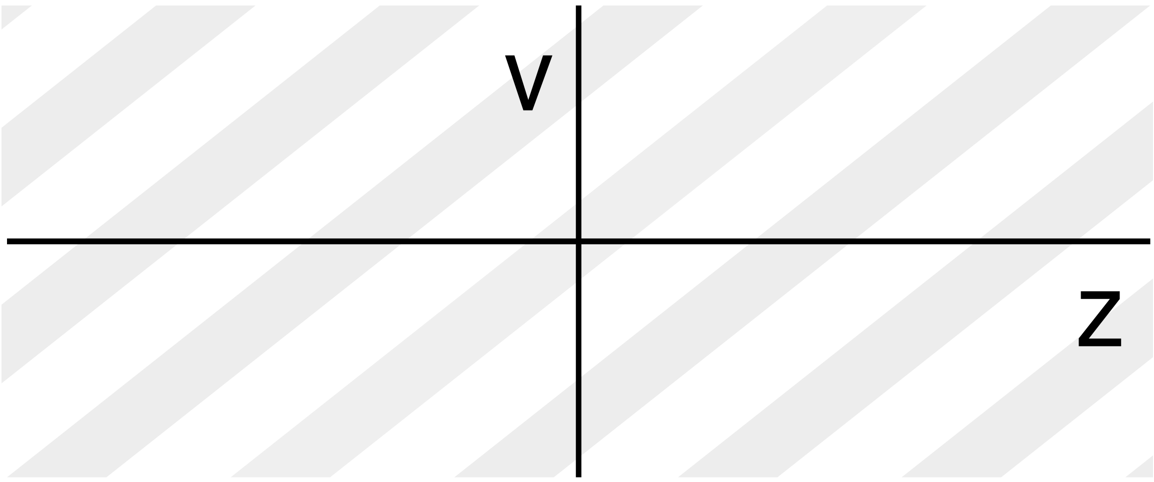

Advected perturbation at time $t = 1$.

Figure 4.1: Illustration of the Plasma Echo. An initial density perturbation is shown in the first picture with spatial structure having wave number $k = 3$. After some time, the perturbation has tilted in phase space, so the perturbation averaged over velocities has decayed.

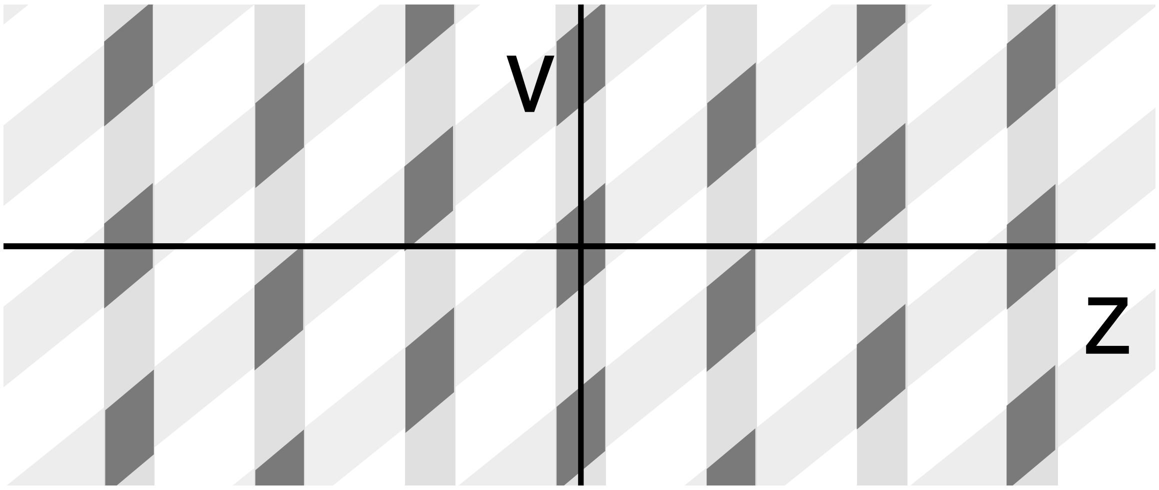

Second perturbation with $k = 2$.

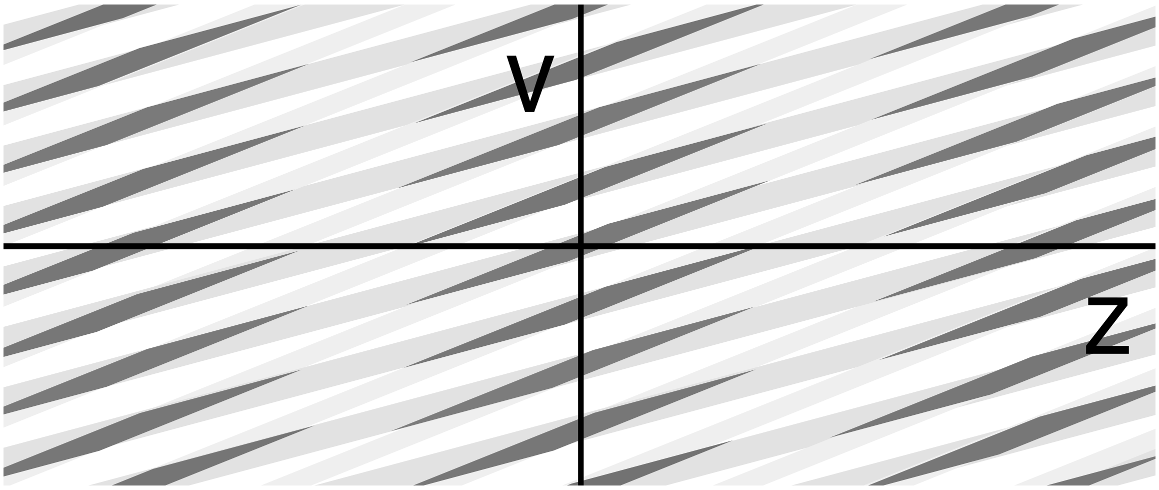

Echo appears at time $t = 3$.

Figure 4.2: Continuation of the plasma echo illustration. A second perturbation with longer wavelength ($k = 2$) is superimposed on the initial perturbation in the first picture. The second-order perturbation is indicated by the dark grey regions. The second picture shows a later time, at which both first-order perturbations have been stretched out in phase space, but the second-order perturbation has reconstituted with a spatial structure with wave number $k = 1$. This reconstituted perturbation at a later time is called *the plasma echo*.

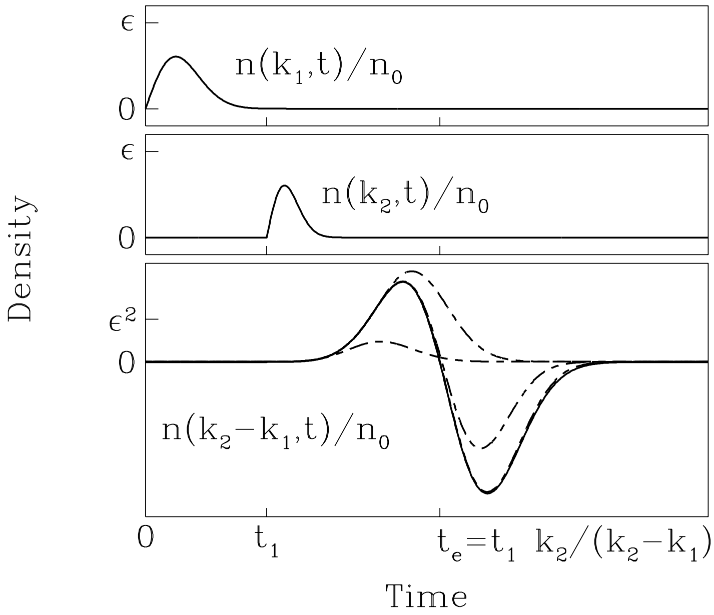

Figure 4.3: The plasma echo response. The density response to two pulses in the potential at wave numbers k_1 and k_2 is plotted here. (For this graph, $\epsilon = 0.01$, $t_1 k_1 v_t = 4$, and $k_2 = 1.7k_1$.) The solid lines denote the exact response for the first-order density components at k_1 and k_2 and the second-order "echo" component at $k_2 - k_1$. The dashed lines indicate the approximate second-order response obtained when 10, 20, 30, and 40 moment equations are used.

Landau damping. The perturbation has not disappeared, however, it has just become convoluted in phase space (phase mixing). If the plasma is then perturbed at a shorter wavelength, a density perturbation will be excited at that wavelength and die away as well. The second perturbation will also interact with the initial perturbation, though, generating a perturbation at the difference wave number that "un-phase-mixes" to appear as a density perturbation at a later time, *the plasma echo.*

Figs. 4.1 and 4.2 present a rough cartoon of the physics of the plasma echo. In Fig. 4.1, an initial perturbation is represented by shaded areas. The streaming of the plasma leads to the usual phase mixing, so the real-space density decays even though the perturbation continues to exist. In Fig. 4.2, a second perturbation is added, which is assumed to interact with the first to produce the second-order contribution indicated by the dark grey regions. At a later time, the second-order contributions line up to produce a spatial density variation at a lower wave number equal to the difference of the two original wave numbers. Note that in the second picture of

Fig. 4.2 the second-order contributions have remained sufficiently localized to produce a perturbation at the low wave number. The criterion for an echo to occur is that the second perturbation occur at a higher wave number than the first. The second-order parts will still line up at a later time if this criterion is not satisfied, but in that case they will have become extremely elongated and produce a small response.

This picture should be only be view as an intuitive guide to the plasma echo, however. In reality, plasmas rarely experience density perturbations of this sort. A more interesting problem, therefore, is to consider the response of the plasma to potential perturbations. The model problem to be considered here is the evolution of a distribution of electrons in one dimension governed by the Vlasov equation (3.5), assuming an externally applied potential of the form

$$\phi(z,t) = -\epsilon_1 \frac{mv_t}{ek_1} \sin(k_1 z)\delta(t-t_1) - \epsilon_2 \frac{mv_t}{ek_2} \sin(k_2 z)\delta(t-t_2), \tag{4.1}$$

and given an initially Maxwellian distribution

$$f(z,v,t=0) = \frac{n_0}{\sqrt{2\pi v_t{}^2}} \exp(-v^2/2v_t{}^2). \tag{4.2}$$

Assuming fixed background ions, and considering the unphysical limit where all of the wavelengths are much shorter than the Debye length, the plasma contribution to the potential may be ignored. Electron fluid equations in this limit are of little physical interest, but this problem contains second-order nonlinearities that can be solved for exactly, and therefore serves as a useful test for the nonlinear performance of fluid moment closures. (Including the self-consistent potential leads to wave propagation that complicates the analysis. The basic second-order effect is the phase de-mixing of second-order perturbations.) O'Neil and Gould (1968) derived the density evolution

$$\begin{aligned} n(z,t) =& n_0 \sum_{l,m} (-i)^{l+m} e^{ik_{lm}z} J_l(\epsilon_1 k_{lm} v_t (t-t_e)) \\ & \times J_m(\epsilon_2 k_{lm} v_t (t-t_2)) \exp(-k_{lm}{}^2 v_t{}^2 (t-t_e)^2/2) \qquad (t > t_2), \end{aligned} \tag{4.3}$$

$$k_{lm} = -lk_1 + mk_2, \tag{4.4}$$

$$t_e = \frac{mk_2 t_2 - lk_1 t_1}{mk_2 - lk_1}, \tag{4.5}$$

where J_n is the usual nth Bessel function and the echo time t_e has been defined for each wave number k_{lm} that enters the response.

Upon expanding the Bessel functions in the echo response (4.3) for small arguments, one notes that the contribution at each wave number scales as $\epsilon_1{}^l \epsilon_2{}^m$. As expected, the contributions at the initially excited wave numbers k_1 and k_2 constitute the first-order contributions to the response. There is a second-order contribution at the sum and difference wave numbers. At the sum wave number $k_1 + k_2$, however,

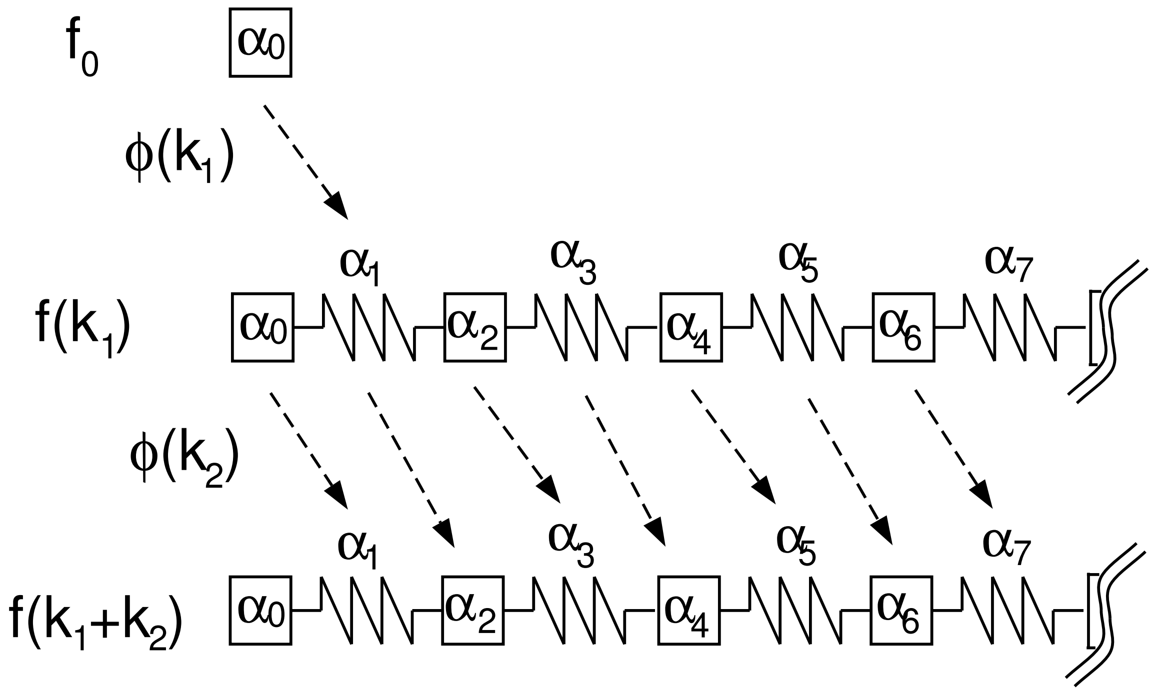

Figure 4.4: The mass–spring system view of the plasma echo. From Section 2.7.2, there is a correspondence between the orthogonal-polynomial moment system and the semi-infinite mass–spring system. Even Hermite moments correspond to the velocities of the masses and odd Hermite moments correspond to the contractions of the springs between them. [See the mass–spring variables in Eq. (2.109).] The initial potential pulse $\phi(k_1)$ couples the background distribution, which has only one nonzero moment a_0, to the wave number k_1 component of the moments (the mass–spring system in the middle of the picture). The perturbation travels as a wave to higher-order moments. The second pulse $\phi(k_2)$ couples the k_1 component of the moments to the $k_1 + k_2$ component of the moments (the mass–spring system at the bottom of the picture). If the echo criterion is satisfied, the perturbation can travel back to lower moments, producing a density echo.

the echo time occurs before the second pulse ($t_e < t_2$), so the exponential term in the response in Eq. (4.3) is very small and the response is negligible. The difference wave number $k_2 - k_1$, on the other hand, has an echo time after the second pulse (possibly much later). Higher-order echoes can appear as well, but this second-order response in the difference wave number is what will be called the *echo response*, and will calculated for closed fluid moment systems in the following section. A typical echo response is plotted in Fig. 4.3 along with the initial density perturbation responsible for the generation of the echo. Note that the echo can occur after both initial perturbations have completely phase-mixed away.

One can also understand the plasma echo in terms of the mass–spring analogy from Chapter 2. Each wave number k has a set of equations in Hermite moments of the form

$$\frac{\partial a_j(k,t)}{\partial t} + ikv_t\left[\sqrt{j}a_{j-1}(k,t) + \sqrt{j+1}a_{j+1}(k,t)\right] = -\sum_{k'} \frac{q\sqrt{j}}{v_t m} a_{j-1}(k-k',t) ik'\phi(k',t), \quad (4.6)$$

which can be mapped to a one-dimensional mass–spring system if the potential interaction is ignored. The zeroth-order distribution only has one nonzero Hermite moment, a_0, so an initial potential pulse excites the first mass in the mass–spring system at wave number k_1. The density perturbation $a_0(k,t)$ dies away in time as the original excitation propagates along the mass–spring chain to higher-order moments. The potential term in the Hermite moment equation (4.6) couples the mass–spring system for wave number k' to that for wave number k through the potential at wave number $k-k'$. [The moment $a_{j-1}(k',t)$ enters the equation for $a_j(k,t)$, so the coupling shifts to the next higher-order moment.] Thus the second potential pulse at wave number k_2 effectively copies that propagated wave in the mass–spring system for wave number k_1 to the mass–spring system for wave number k_1+k_2. If the echo condition is satisfied, then k_1+k_2 has sign opposite to that of k_1 and the new mass–spring wave travels in the opposite sense of the original, transferring energy back to lower moments and eventually to the density $a_0(k_1+k_2,t)$. The mass–spring wave then bounces off the free boundary condition at the first mass a_0, which is attached to nothing on the left, and the echo decays as the wave travels back to higher-order moments. This picture is illustrated in Fig. 4.4.

4.2 The Echo in Closed Moment Systems

The potential failing of a system that evolves a finite number of moments is clear from the picture in Fig. 4.4. If one attempts to model a pair of pulses such as those in Eq. (4.1) for an interaction time $t_2 - t_1$ that is too long, then the the first-order perturbation wave will have hit the end of the chain of moments and been dissipated by the closure model. The closed moment system will therefore fail to produce the predicted second-order response in this case. Studies of series solutions of the Vlasov equation (Armstrong et al. 1970) noted that simulations could only capture the complete nonlinear physics for times $t < \sqrt{m}/(kv_t)$, where m is the number of coefficients in the series used. After that time, the effect of the truncated coefficients is no longer negligible. Since the Hermite moment equations are equivalent to the Hermite series approach, one expects the same limitation for fluid equations.

Solution of the application of the potential pulses in Eq. (4.1) to the closed Hermite moment system discussed in Section 3.3 is very straightforward. The pulses will produce nonzero Fourier components for wave numbers 0, k_1, k_2, and $\pm k_1 \pm k_2$ only. The n-moment system solution for the echo can therefore be found by evolving the

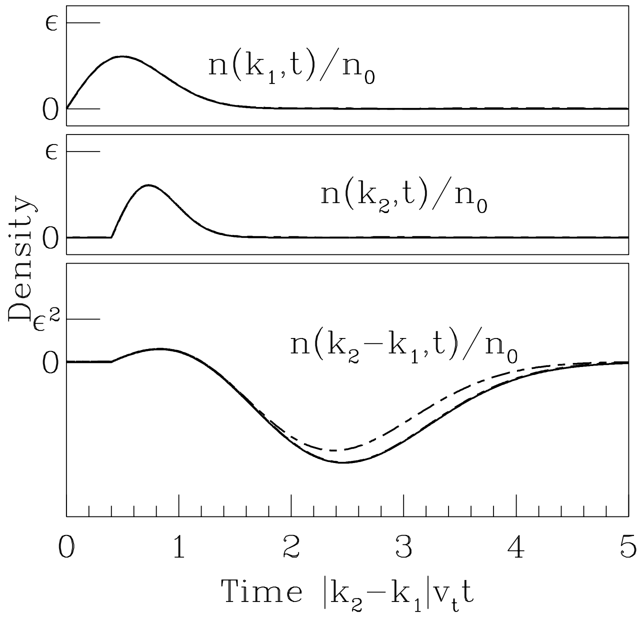

Figure 4.5: The plasma echo density response for short interaction time $(t_2-t_1)k_1v_t = 0.8$. The exact density responses are plotted with solid lines and there are two sets of dotted lines indicating the responses for the 10 Hermite moment system with the $q = 3$ closure and $q = 9$ closure. Both choices of closure give the correct first-order response. The $q = 3$ closure matches the second-order response almost exactly, however, while the $q = 9$ closure departs slightly from the correct answer.

equations

$$\frac{\partial}{\partial t}a_0(k_1,t)+ik_1v_ta_1(k_1,t) = 0, \tag{4.7}$$

$$\frac{\partial}{\partial t}a_1(k_1,t)+ik_1v_t\left[a_0(k_1,t)+\sqrt{2}a_2(k_1,t)\right] = n_0\frac{\epsilon_1}{2}\delta(t-t_1), \tag{4.8}$$

$$\frac{\partial}{\partial t}a_j(k_1,t)+ik_1v_t\left[\sqrt{j}a_{j-1}(k_1,t)+\sqrt{j+1}a_{j+1}(k_1,t)\right] = 0 \quad (2 \le j < n), \tag{4.9}$$

$$\frac{\partial}{\partial t}a_j(k_1-k_2,t)+i(k_1-k_2)v_t\left[\sqrt{j}a_{j-1}(k_1-k_2,t)+\sqrt{j+1}a_{j+1}(k_1-k_2,t)\right]$$
$$= \sqrt{j}a_{j-1}(k_1,t)\frac{\epsilon_2}{2}\delta(t-t_2) \qquad (0 \le j < n), \tag{4.10}$$

along with the closure condition discussed in Section 3.2 for the unresolved moments $a_n(k_1,t)$ and $a_n(k_1-k_2,t)$. The results can then be compared to the k_1-k_2 component of the exact solution (4.3).

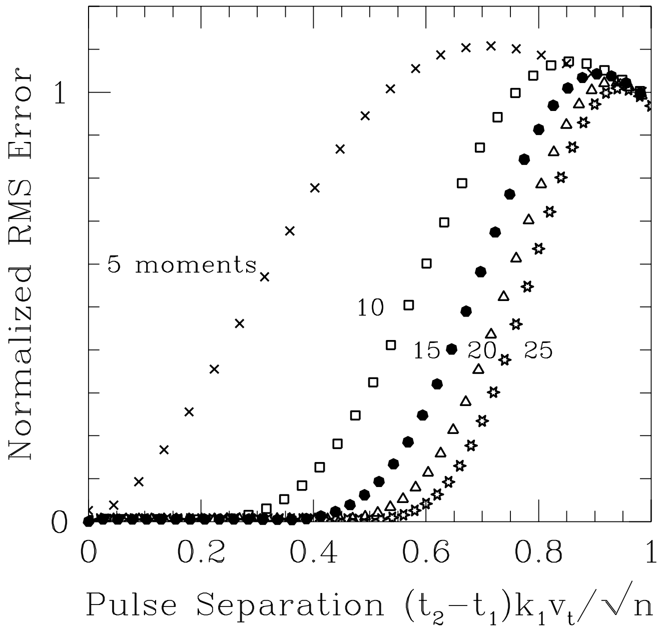

Figure 4.6: The normalized root-mean-squared error of the second order response $\int_0^\infty [n^{\rm a}(k_2 - k_1, t) - n(k_2 - k_1, t)]^2\, dt / \int_0^\infty n(k_2 - k_1, t)^2\, dt$ is plotted against the normalized interaction time $(t_2 - t_1)k_1 v_t/\sqrt{n}$ for closed Hermite moment systems with $n = 5$, 10, 15, 20 and 25 moment equations.

Some results are displayed for a fairly long interaction time $[k_1 v_t(t_2 - t_1) = 4]$ in Fig. 4.3. With 40 Hermite moments the echo is reproduced almost exactly in that case, but for 10 moments the system produces almost no echo. The 10-moment system fails for this example because the initial perturbation has become sufficiently convoluted after this interaction time that it is no longer represented by the first 10 Hermite moments. In Fig. 4.5, the results for a shorter interaction time $(k_1 v_t[t_2 - t_1] = 0.8)$ are displayed for the 10 Hermite moment system, which is successful in this case. Two choices of q, the number of times the linear response is matched in the $\omega \to 0$ limit, are illustrated in this figure. For $q = 3$, the dotted line for the second-order response is indistinguishable from the exact response. For $q = 9$ there is some error, although the simulation still gives a reasonable response. Both choices of q give an excellent fit to the linear theory, so for large numbers of moments it is probably best to take a small value of q. (The linear theory converges very slowly for $q = 1$, however, so the choices $q = 2$ or $q = 3$ are better.)

The mean-squared error in the second-order response was calculated for a number of closed moment systems with $q = 3$ for various interaction times. The results are plotted in Fig. 4.6. For a sufficiently large number of moments, there is almost no error in modeling the second-order response for interaction times $(t_2-t_1)k_1v_t < \sqrt{n}/2$, and there is a transition of increasing error until $(t_2-t_1)k_1v_t > \sqrt{n}$, at which point the closed moment system gives virtually no second-order response, so the error is 1. These results indicate, however, that a small number of moment equations can model the second-order response for very short interaction times only.

4.3 Relation to Perturbation Expansions

It is instructive to derive the response for this model problem perturbatively. Assume the potential is small, $\phi(z,t) = \epsilon\psi(z,t)$, and expand the distribution formally in a perturbation series

$$f(z,v,t) = f_0(z,v,t) + \epsilon f_1(z,v,t) + \epsilon^2 f_2(z,v,t) + \cdots . \tag{4.11}$$

Solving the Vlasov equation (3.5) term by term with the potential given by Eq. (4.1) yields the hierarchy of equations

$$\frac{\partial f_0}{\partial t} + v\frac{\partial f_0}{\partial z} = 0 \tag{4.12}$$

$$\frac{\partial f_1}{\partial t} + v\frac{\partial f_1}{\partial z} = \frac{q}{m}\frac{\partial \psi}{\partial z}\frac{\partial f_0}{\partial v}, \tag{4.13}$$

$$\frac{\partial f_2}{\partial t} + v\frac{\partial f_2}{\partial z} = \frac{q}{m}\frac{\partial \psi}{\partial z}\frac{\partial f_1}{\partial v}, \tag{4.14}$$

$$\vdots$$

Assuming a Fourier decomposition with periodic boundary conditions, $\psi(z,t) = \sum_k \exp(ikz)\psi_k(t)$ and $f_i(z,v,t) = \sum_k \exp(ikz) f_i(k,v,t)$, these equations are easily solved to give the evolution of each term in the expansion,

$$f_0(z,v,t) = \frac{n_0}{\sqrt{2\pi v_t{}^2}}\exp(-v^2/2v_t{}^2), \tag{4.15}$$

$$f_1(k,v,t) = \frac{q}{m}\int_0^t e^{-ikvt_1} ik\psi(k,t-t_1)\frac{\partial}{\partial v}f_0(v)\,dt_1, \tag{4.16}$$

$$\begin{aligned} f_2(k,v,t) = &\frac{q}{m}\int_0^t \sum_{k'} e^{-ikvt_1} i(k-k')\psi(k-k',t-t_1) \\ &\times \frac{\partial}{\partial v} f_1(k',v,t-t_1)\,dt_1. \end{aligned} \tag{4.17}$$

The density response therefore expands as $n(z,t) = n_0 + \epsilon n_1(z,t) + \epsilon^2 n_2(z,t) + \cdots$, and one finds that the second component is

$$\begin{aligned} \epsilon^2 n_2(k,t) = &n_0 \int_0^t \int_0^{t-t_2} \sum_{k'} \frac{q^2}{m^2 v_t{}^2}(k-k')\phi(k-k',t-t_2) \\ &\times k'\phi(k',t-t_2-t_1)\mathsf{R}_2(kv_tt_2,k'v_tt_1)\,dt_1\,dt_2, \end{aligned} \tag{4.18}$$

where the second-order response function is

$$\mathsf{R}_2(\tau_2,\tau_1) = \tau_2(\tau_1+\tau_2)\exp(-(\tau_1+\tau_2)^2/2). \tag{4.19}$$

This second-order response gives the density at time t caused by the potential at times $t-t_2$ and $t-t_2-t_1$. The response is typically exponentially small unless the argument $\tau_1+\tau_2$ vanishes, which will occur if k and k' have opposite signs. (This is equivalent to the echo criterion that the wave number $k-k'$ of the second pulse is larger than that of the first pulse, k'.)

Note that the echo response increases linearly with the delay t_1 between the two potential pulses. The exact nonlinear response in Eq. (4.3), on the other hand, replaces $\epsilon^2\mathsf{R}_2(\tau_1,\tau_2)$ with $J_1(2\epsilon\tau_1)J_1(2\epsilon(\tau_1+\tau_2))\exp(-(\tau_1+\tau_2)^2/2)$. Thus, the second-order expansion is only valid for analyzing delay times such that $\epsilon k v_t t_1 \ll 1$. The second-order perturbation is a function of the velocity derivative of the first-order perturbation. Even when the first-order perturbation is rigorously small, the derivatives increase with time as the perturbation becomes convoluted in phase space. One should be careful, therefore, in interpreting the long-time behavior of any second-order perturbation theory.

The difference between kinetic theory and Landau-fluid theory that was demonstrated by Mattor (1992) can be understood by looking at the Hermite moment expansion. From the picture in the previous section illustrated in Fig. 4.4, one can see that the second-order density response can be decomposed as the linear density response to initial conditions in higher-order moments that are in turn linear responses to an initial perturbation in the first moment $a_1(k_1)$. In terms of the general orthogonal-polynomial responses defined in Eq. (2.62), the second-order echo response can be decomposed as

$$\mathsf{R}_2(\tau_2,\tau_1) \propto \sum_{j=0}^{\infty} \mathsf{R}_{0,j+1}(\tau_2)\sqrt{j}\,\mathsf{R}_{j,1}(\tau_1). \tag{4.20}$$

The errors introduced in the second-order response for a truncated moment system with closure are fairly complicated then, since we must consider the errors introduced in all the linear responses of the form $\mathsf{R}_{0,j+1}$ and $\mathsf{R}_{j,1}$. The theory from Chapter 2 indicates that the Laplace transform of all the components of the linear response matrix will eventually converge, given enough moments. From Result 3, if the first p closure coefficients are set to zero for $p \geq 1$, then the errors in $\mathsf{R}_{0,j+1}$ for $j+1 \leq p$ and all $\mathsf{R}_{j,1}$ are all related to one another by factors of Hermite polynomials. For the Maxwellian (Gaussian) case, the response functions converge with increasing numbers of moments for any fixed choice of q, the number of times the response is matched in the $\omega \to 0$ limit. Thus a set of closures exists for which $n \to \infty$ and $p \to \infty$, so that all the response functions eventually converge.

For a given closed moment system with a sufficiently large number of moments n, therefore, the main source of error in the second-order response will come from the truncation of the decomposition (4.20) due to the fact that moments with $j > n$ are not modeled. (The responses that are modeled are modeled very well with large numbers of moments.) Assume that the linear time response of each moment could be modeled exactly. The Hermite moments are expanded in the formal series $a_j(z,t) = a_j^0(z,t) + \epsilon a_j^1(z,t) + \epsilon^2 a_j^2(z,t) + \cdots$, where $a_j^0(z,t)$ is the jth Hermite moment of $f_0(z,v,t)$ and so on. Expanding the first-order response (4.16) in terms of the first n Hermite moments yields an approximation to the first-order part of the density:

$$\begin{aligned} f_1(k,v,t) &\sim \sum_{j=0}^{n-1} a_j^1(k,t) \frac{1}{\sqrt{2^j j!}} H_j(v/\sqrt{2}v_t) \frac{1}{\sqrt{2\pi v_t{}^2}} \exp(-v^2/2v_t{}^2) \\ &= \sum_{j=0}^{n-1} \frac{1}{\sqrt{2^j j!}} H_j(v/\sqrt{2}v_t) \frac{n_0}{\sqrt{2\pi v_t{}^2}} \exp(-v^2/2v_t{}^2) \\ &\quad \times \frac{q}{m} ik \int_0^t \psi(k, t-t_1) \frac{-1}{v_t\sqrt{j!}} \left[(-ikv_t t_1)^{j+1} \right. \\ &\qquad \left. + j\,(-ikv_t t_1)^{j-1} \right] e^{-(kv_t t_1)^2/2}\, dt_1. \end{aligned} \tag{4.21}$$

By inserting this approximation into the equation for the second-order component of the density equation (4.17), one obtains an approximation to the density response,

$$\begin{aligned} \mathsf{R}_2^{\mathrm{a},n}(\tau_2,\tau_1) &\sim \tau_2\,(\tau_2+\tau_1) \exp(-(\tau_1{}^2+\tau_2{}^2)/2) \\ &\quad \times \left[\sum_{l=0}^{n-1} \frac{1}{l!} (-\tau_2\tau_1)^l - \frac{\tau_2(-\tau_2\tau_1)^{n-1}}{\tau_2+\tau_1} \right]. \end{aligned} \tag{4.22}$$

Using a finite set of moments effectively replaces the term $\exp(-\tau_2\tau_1)$ in the second-order response (4.19) with a Taylor series in $\tau_2\tau_1$. For small τ_1 and small τ_2, the Taylor series is a good approximation. For large τ_1 and τ_2, the exponential terms in the approximate echo response (4.22) dominate to give an exponentially small response. This result is a good approximation to the true response (4.19) except near the line $\tau_1 = -\tau_2$ where the combined exponential terms are $\mathcal{O}(1)$. [When the argument of $\exp(-\tau_2\tau_1)$ is positive it can balance the other exponential terms.] Since the n-term Taylor series of $\exp(x)$ is a good approximation out to $|x| \sim n$, this approximate second-order response is valid for interaction times $|\tau_1\tau_2| < n$. The response is exponentially small except where $\tau_1 \sim -\tau_2$, so this condition corresponds to $(kv_t t_1)^2 < n$, which is essentially the recurrence-time condition discussed in the previous section.

This response is very similar to that obtained for second-order perturbations in weak-turbulence theory (Mattor 1992). The Laplace transform of the second-order response in Eq. (4.18) can be written as

$$\begin{aligned} \epsilon^2 n_2(k,\omega) =& \frac{n_0}{2\pi} \int_{-\infty}^{\infty} \sum_{k'} \frac{q^2}{m^2 v_t{}^2} (k-k')\phi(k-k',\omega_1) k'\phi(k',\omega-\omega_1) \\ & \times \frac{1}{4|k||k'|v_t{}^2} \widehat{\mathsf{R}}_2 \left(\frac{\omega}{\sqrt{2}|k|v_t}, \frac{\omega-\omega_1}{\sqrt{2}|k'|v_t} \right) d\omega_1, \end{aligned} \tag{4.23}$$

where the transformed second-order response is given by

$$\begin{aligned}\widehat{\mathsf{R}}_2(\zeta_2,\zeta_1) &= \int_0^\infty \int_0^\infty e^{i\zeta_2\tau_2} e^{i\zeta_1\tau_1} \mathsf{R}_2\left(s\frac{\tau_2}{\sqrt{2}}, s'\frac{\tau_1}{\sqrt{2}}\right) d\tau_1\, d\tau_2 \\ &= s\frac{\partial}{\partial\zeta_2}\left(s'\frac{\partial}{\partial\zeta_1} + s\frac{\partial}{\partial\zeta_2}\right) \frac{sZ(\zeta_2) - s'Z(\zeta_1)}{s\zeta_2 - s'\zeta_1}.\end{aligned} \tag{4.24}$$

(To simplify the expression, the sign variables $s = k/|k|$ and $s' = k'/|k'|$ have been introduced.) The series expansion from Eq. (4.22), on the other hand, gives approximately the response

$$\widehat{\mathsf{R}}_2(\zeta_2,\zeta_1) \approx s\frac{\partial}{\partial\zeta_2}\left(s'\frac{\partial}{\partial\zeta_1} + s\frac{\partial}{\partial\zeta_2}\right) \left[\sum_{j=0}^{n-1} \frac{1}{j!}\left(\frac{1}{2}s\frac{\partial}{\partial\zeta_2}s'\frac{\partial}{\partial\zeta_1}\right)^j\right] sZ(\zeta_2)s'Z(\zeta_1). \tag{4.25}$$

Mattor (1992) pointed out that the Landau-fluid approximation to the response remains finite for all ζ_1 and ζ_2 and therefore misses the resonant behavior in Eq. (4.23) when $ss' = -1$ and $\zeta_1 \to -\zeta_2$. It is worth pointing out, however, that this approximation converges with increasing numbers of moments. Near the resonance, however, this expression (4.25) converges extremely slowly with increasing n, the number of moments.

4.4 Limitations of Moment Equations

The time response for the linear Vlasov equation is modeled extremely well by Landau-fluid equations with as few as four moment (Hammett et al. 1992). The echo phenomenon, however, reconstructs information from the entire velocity-dependent part of the distribution function. Hence, although a plasma echo is essentially a linear response to the perturbation of a linear response, simply getting the linear response correct is not sufficient to model the echo. The ability of any set of moment equations to model a plasma echo is limited by the amount of velocity-dependent distribution information that is contained in the finite number of moments kept.

Previous studies using truncated Hermite series expansions noted this time limit as well. For example, Armstrong et al. (1970) were forced to terminate their simulations at a time $t < \sqrt{N}/kv_t$. Part of this time restriction arose from their choice of closure $\alpha_N(x,t) = 0$, which effectively reflects information back to lower moments, causing recurrence. With the linear closure used here, perturbations will decay correctly according to the linear theory without recurring. What is missed, however, is the interaction between waves separated by times larger than $\sim \sqrt{n}/kv_t$. In reality, however, a second interaction cannot occur for arbitrarily large separation times. Echoes can only occur in an almost collisionless plasma, since they depend on delicate convolutions in velocity space that are easily destroyed by collisions.

By considering the simple collision model in equation 3.5, Su and Oberman (1968) found that a free-streaming perturbation of wave number k is damped by an exponential term of the form $\exp(-\nu k^2 {v_t}^2 t^3/3)$. This decay implies that for separation times of the order

$$t_2 - t_1 \sim \left(\frac{1}{\nu {k_1}^2 {v_t}^2}\right)^{1/3}, \tag{4.26}$$

there will be no second-order response when the effect of collisions is taken into account. The number of moments required to model this separation time scales as $N \sim (t_2 - t_1) v_t k_1$, so a rough estimate of the number of moments N needed to model all second-order effects that can occur is given by

$$N \sim \left(\frac{k v_t}{\nu}\right)^{2/3}. \tag{4.27}$$

4.5 Summary

The dissipative Landau-fluid closure has a significant impact on the linear physics of closed moment systems. A model nonlinear problem, the plasma echo, was considered as a simple nonlinear test of the closure. The plasma echo is essentially the second-order component of the nonlinear response expanded in the limit of small perturbations. The second-order response has an exact solution (4.3) in the limit where the self-consistent potential is dropped. This exact solution was used to gauge the weakly nonlinear performance of moment systems with closure.

In contrast to the linear picture, the choice of linear closure does not have a large impact on the second-order response. (See Fig. 4.5.) The number of moments simulated, however, is an essential factor in resolving second-order effects. The results summarized in Fig. 4.6 that modeling the second-order response for interaction time $t_2 - t_1$ requires $n \sim [(t_2 - t_1) k_1 v_t]^2$ moments. A simple model of the rate of decay of perturbations due to a finite collision rate ν indicates that $n \sim (k v_t/\nu)^{2/3}$ moments are sufficient to resolve all second-order effects.

Clearly this second-order streaming nonlinearity cannot be accurately modeled with small numbers of moments. This effect is second-order, however, so for perturbations that are small with respect to the background, the unresolved density perturbations should be a small correction.